

CONCEPTS FOR MORE FLEXIBLE UED/UEM OPERATION*

J.W. Lewellen[†], Los Alamos National Laboratory, Los Alamos, NM, United States
 J. Smedley, SLAC National Accelerator Laboratory, Menlo Park, CA, United States

Abstract

Ultrafast electron diffraction and microscopy (UED/UEM) has advanced beyond the proof-of-concept stage into the realm of instrumentation, particularly for pump-probe type experiments. To date, most UED/UEMs have been constructed around high-gradient radiofrequency (RF)-driven electron guns originally designed as X-FEL beam sources.

A UED/UEM system driven by a CW beam source, either normal- or superconducting, offers several potential performance benefits over high-gradient pulsed beam sources. These include the ability to operate at much higher average repetition rates, and the ability to extend measurement times beyond $O(1 \mu\text{s})$. If a quarterwave-type beam source is used, there is an additional possibility to vary the time between probe pulses by other than an RF period.

In this paper we present the basis for this assertion, discuss implications for detectors, and consider also utilization of probe electron beams at different beam energies.

INTRODUCTION

In the context of UED/UEM, the RF gun often serves as the probe source in pump-probe type experiments, with a laser pulse serving as the pump. In the case of a single pump and single probe, e.g. exploring a reversible ultrafast phenomenon, varying the time delay between the two is relatively straightforward via a combination of optical delay lines and timing systems. A UED/UEM based around a conventional, multicell, high-frequency ($> 1 \text{ GHz}$) normal-conducting RF gun [1] is very well matched to the requirements of such experiments.

There are, however, classes of experiments in which the phenomenon being probed is non-reversible, leading to the desire to follow a single “pump” event with multiple probe pulses, with a pulse train potentially extending out to the ms regime [2,3]. In other cases, several probe pulses with relatively short (ns-scale) but time-variable separation may be desired [4]. A CW-capable RF gun is clearly a good choice for the former class of experiments. For the latter, a single-cell, low-frequency RF gun offers advantages over a high-frequency multicell gun.

RF GUN CHARACTERISTICS

For the particular application of UED/UEM, it is helpful to consider, as the primary distinction, high-frequency multicell versus low-frequency single-cell guns.

High-frequency RF guns, or those operating at an RF frequency of 1 GHz or greater, typically are multi-cell,

consisting of a cathode cell and one or more “full” cells (or cells with length of $\frac{1}{2}$ the free-space wavelength). The cathode cell length is typically optimized according to the gun’s design operating point but is usually on the order of $\frac{1}{4}$ of a free-space wavelength [1]. Most such guns are pulsed, with RF pulse durations on the order of 1-10 μs , and repetition rates on the order of 10-100 Hz. (There are of course exceptions, including the long-pulse Euro X-FEL gun [5], the LANL 700-MHz CW gun [6], and a number of n.5-cell, 1.3-GHz SRF guns, including the HZDR SRF gun [7,8].) For purposes of our discussion, the common feature among these guns is beam dynamics generally in accord with “classic” Carlsten / Kim / Rosenzweig / Serafini beam dynamics [9].

In contrast, consider low-frequency single-cell guns. As a class, these guns typically are designed to operate in the 100-200 MHz range (“VHF”), and have a cavity geometry that can be described as either “quarterwave” (QW) (in analogy to hadron accelerator cavities) or extremely reentrant. The accelerating gaps are typically relatively very short, on the order of 0.05-0.1 of a free-space wavelength. Such guns are usually intended to operate CW. In a beam dynamics sense, they are more similar to DC guns than they are to high-frequency multicell RF guns [10].

LFCW-CAPABLE RF GUNS

To date, most UED/UEM experiments and facilities have been designed around high-frequency multicell RF guns, for instance [11] (with the LBNL facility [12] being a notable exception). This is unsurprising given the relative body of experience, and the number of such guns designed, built and tested, compared to low-frequency designs.

There are considerations that would seem to argue against using low-frequency CW-capable (LFCW) guns in a small facility. Compared to high-frequency guns, LFCW guns typically provide a lower on-cathode accelerating gradient, meaning they are more restrictive in terms of tradeoffs between bunch charge, emission duration, and emission spot size (and thus thermal emittance). The ability to operate CW has implications for facility shielding, as well as cooling (for normal-conducting) or cryogenic (for superconducting) requirements. Facility and operational considerations also include thermal loading (e.g. on RF windows), the need to maintain particle-free beamline practices, and experimental background in the form of dark current.

LFCW-type RF guns do offer two significant benefits for UED/UEM application, however: the ability to accommodate measurements that need to extend for durations longer than 1 – 10 μs (thanks to CW operation); and the ability to provide variable beam pulse spacing within a single RF period (thanks to DC gun-like beam dynamics).

* Work performed under the auspices of the US Department of Energy by Triad National Security under contract 89233218CNA000001.

† jwlewellen@lanl.gov

(report LA-UR-24-24149)

Current normal-conducting designs, such as the LBNL APEX gun and the LCLS-II beam source, typically operate at up to 20 MV/m on the cathode. The SLAC/MSU SRF gun [13] is designed to operate at 30 MV/m on the cathode, and a prototype cavity has demonstrated this gradient. SRF guns also have intrinsically outstanding vacuum, which should aid in preserving cathode lifetime.

VARIABLE BEAM PULSE TIMING

Any RF gun should in principle be able to provide multiple electron beam pulses, at the “natural” spacing at the RF frequency. The beam is launched at the same phase of the RF field; beam parameters should be the same shot-to-shot, and the delay between the pulses is n / f , where n is an integer and f is the RF frequency. For instance, a C-band gun ($f=5.712$ GHz) can “naturally” make bunches spaced at $n^*(175$ ps), for (assuming a 1- μ s RF “flattop”) $n < 5700$. In contrast, a CW VHF gun ($f \sim 200$ MHz) can naturally make beam bunches spaced at ~ 5 ns; as the gun is CW, $n \sim \infty$.

A question arises: what if a shorter, or simply different, bunch spacing is required? To start to answer this question, we assume two boundary conditions: the two beams should be at the same energy, and should have the same Twiss parameters, such that they have identical behavior in any downstream transport line.

Beam Launch Phase Selection

Figure 1 and Figure 2 show, respectively, the beam energy versus launch phase (0 degrees is defined as the E-field zero crossing on the cathode) for a generic 1.5-cell S-band photoinjector with an on-axis field approximated by $\frac{3}{4}$ of a sine wave and 100 MV/m peak field on the cathode; and for the SLAC/FRIB QW SRF gun with a 30-MV/m peak cathode gradient. Both figures indicate the range in time over which we might expect to generate two electron beam pulses with the same beam energy, within a single RF period.

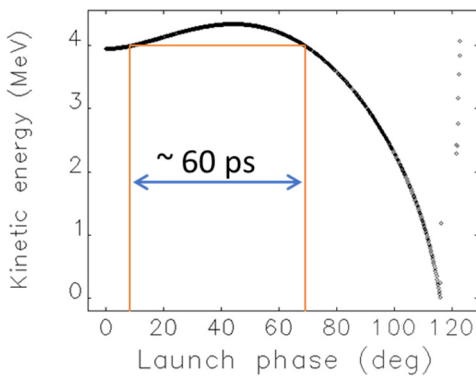


Figure 1: Beam kinetic energy vs. launch phase (black dots) for a generic 1.5-cell S-band RF gun.

We note that this approach does not provide completely arbitrary timing between beam pulses. Rather, the separation between beam pulses of equal energy can be

$$\left(n \pm \frac{\Delta\Phi}{2\pi} \right) \tau,$$

where n is an integer ≥ 0 , τ is the RF period, and $\Delta\Phi/2\pi$ is the fraction of an RF period over which two equal-energy beams can be generated. For the S-band gun, $\Delta\Phi$ is approximately 60 degrees; for the SLAC/FRIB QW gun, $\Delta\Phi$ is approximately 120 degrees.

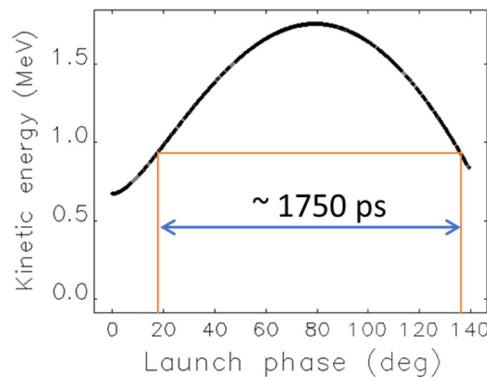


Figure 2: Beam kinetic energy vs. launch phase (black dots) for the SLAC/FRIB SRF gun.

Satisfying the first boundary condition, therefore, is straightforward; two launch phases are chosen that provide the desired pulse separation, and have the same beam energy.

Mismatch Calculation

For a given desired time separation Δt between beam pulses arriving at the exit of the gun (or equivalently, launch phase separation $\Delta\phi$ providing that arrival time separation), two launch phases $\phi_{1(2)}$ are identified that provide the same beam kinetic energy E_k . The transverse Twiss parameters $\alpha_{1(2)}$ and $\beta_{1(2)}$ of the beams generated at $\phi_{1(2)}$ can be compared to determine the relative mismatch of the beams to each other, or to a transport line. These parameters are illustrated in Figure 3.

The mismatch parameter ζ is defined as [14]

$$\zeta \equiv \frac{1}{2} \left(\beta_1 \frac{1 + \alpha_2^2}{\beta_2} - 2\alpha_1\alpha_2 + \beta_2 \frac{1 + \alpha_1^2}{\beta_1} \right) \geq 1,$$

(where the equation is rewritten to explicitly eliminate the γ parameter) and characterizes the relative alignment of the two beams’ ellipses in transverse phase space. For two perfectly matched beams (e.g. identical Twiss parameters), $\zeta=1$. Note that the mismatch does not depend on the beam emittance; two beams with different emittances can be perfectly matched.

To assess the second boundary condition we impose, we calculate the mismatch parameter between beams of equal energy, as a function of the difference in launch phases for that energy. The General Particle Tracer (GPT) [15] code was used to simulate both guns in as simple a model space as possible to perform an initial assessment. Only RF fields were included. “Short” bunches of ~ 1 ps were generated. Neither space charge effects nor external focusing (e.g. solenoids) were included. The bunch distributions were saved several cm past the nominal end of the guns’ cavities where the on-axis field falls to ~ 0 . Finally, the

sddsanalyzebeam program (distributed with **elegant** [16]) was used to calculate the beam parameters.

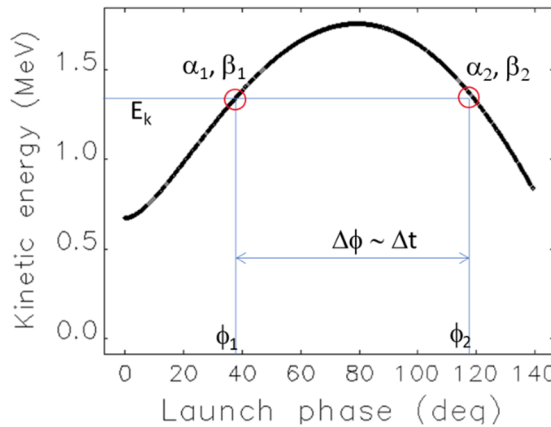


Figure 3: Parameters for calculating mismatch.

The mismatch parameter vs. launch phase is shown in Figure 4. Note that the horizontal scale is in phase (degrees), not time. In short, the SLAC/FRIB QW SRF gun maintains a low mismatch over the entire range of accessible pulse spacings; the generic S-band gun, in contrast, shows significant mismatch at all but the shortest pulse-to-pulse spacings.

The results reported above for a “generic” 1.5-cell S-band gun are similar to those obtained when using the “as-built” field of a SLAC/BNL/UCLA 1.6-cell photoinjector. In fact, the “generic” design has a somewhat wider phase window over which equal beam energies can be obtained, and somewhat less arrival time compression, than the 1.6-cell SLAC/BNL/UCLA gun optimized as an X-FEL beam source.

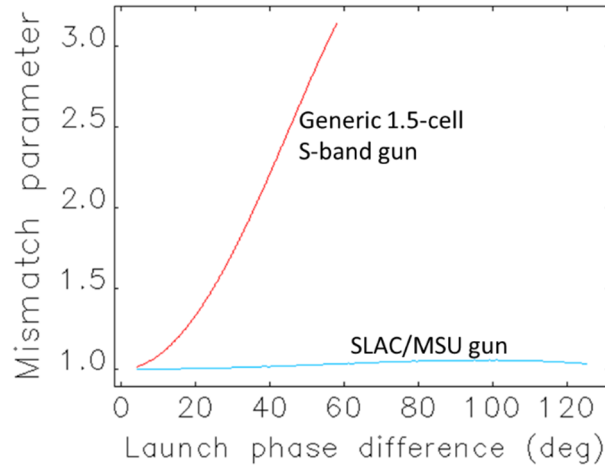


Figure 4: Mismatch parameter vs. launch phase difference.

NEXT STEPS

Depending on the pulse separation, the ability to resolve two separate pulses on the same detector may prove challenging. Several methods exist for separating the pulses spatially to allow multiple detectors, or two different regions of the same detector, to be used.

Active approaches, e.g. with a deflector cavity, will likely pose additional restrictions on pulse-to-pulse

separation due to phase-matching requirements, add additional considerations re timing jitter, phase and amplitude stability, etc., and require additional high-power RF systems.

Alternately, an energy difference could be used to passively separate the pulses, e.g. via dispersion through a bending magnet. This approach would result in a more complicated transport line, but also ease mismatch tolerance as separating the bunches via energy would allow, at least to some extent, independent focusing control. Comparing Figure 1 to Figure 2, the SLAC/FRIB SRF gun shows an approximate factor of 3 difference in accessible beam energies. While the generic 1.5-cell gun nominally has a wider range, beam quality generally suffers at high launch phases, and sensitivity to jitter would be increased. We intend to develop several “straw-man” concepts, such as the one shown in Figure 5, as a means to explore the parameter space, define beam requirements (e.g. energy spread limits) and develop useful metrics for characterizing performance.

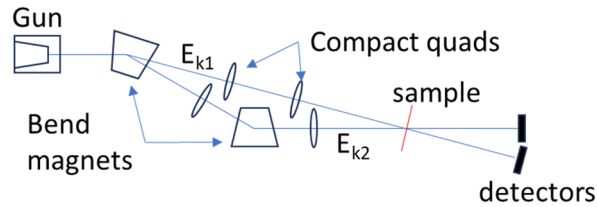


Figure 5: Concept for a 2-energy, 2-detector UED beam-line. In this case the beam energy $E_{k1} > E_{k2}$.

CONCLUSIONS

We considered the ability of both high-frequency multi-cell, and low-frequency single-cell, photoinjectors to generate beams with variable pulse-to-pulse timing, using a generic 1.5-cell S-band gun, and the SLAC/FRIB superconducting quarterwave gun, as exemplars.

Within a defined maximum phase separation, both types of gun can generate two beam pulses with equal beam energy. In the case of the SLAC/FRIB gun, the transverse phase spaces of the pulses remain reasonably well-matched throughout the range of achievable pulse-to-pulse intervals. In contrast, the 1.5-cell S-band gun exhibits very strong growth in the mismatch parameter as pulse separation increases.

ACKNOWLEDGEMENTS

We thank Ting Xu and the SLAC/MSU SRF gun team for interesting discussions and insights. We are grateful to Fernando Sannibale’s initial development efforts on VHF-type RF guns, and advocacy for their potential. We also thank Xijie Wang for his pioneering efforts in developing both RF guns and RF gun-based UED/UEMs.

REFERENCES

- [1] D.H. Dowell, “Chapter 2: Normal Conducting RF Injectors,” in *An Engineering Guide to Photoinjectors*, T. Rao and D.H. Dowell, Eds., 2013. ISBN-13: 978-1481943222

- [2] R. L. Sheffield, C. W. Barnes, M. A. Bourke, R. W. Garnett, M. S. Gulley, and A. J. Taylor, "Pre-Conceptual Design Requirements for an X-Ray Free Electron Laser for the MaRIE Experimental Facility at LANL", in *Proc. PAC'11*, New York, NY, USA, Mar.-Apr. 2011, paper THP163, pp. 2417-2419.
- [3] H.-J. Ziock, "The proton radiography concept," Los Alamos National Report LA-UR-98-1368 (1998).
- [4] for example, the description of the LLNL Dynamic Transmission Electron Microscope (<https://pls.llnl.gov/resources/dynamic-transmission-electron-microscope>) and references thereon.
- [5] G. Vashchenko *et al.*, "Emittance Measurements of the Electron Beam at PITZ for the Commissioning Phase of the European X-FEL", in *Proc. FEL'15*, Daejeon, Korea, Aug. 2015, pp. 285-288. doi:10.18429/JACoW-FEL2015-M0D04
- [6] D. C. Nguyen *et al.*, "Overview of the 100mA average-current RF photoinjector," *Nucl. Instrum. Methods Phys. Res., Sect. A*, vol. 528, no. 1-2, pp. 71-77, Aug. 2004. doi:10.1016/j.nima.2004.04.021
- [7] H. Vennekate, A. Arnold, P. N. Lu, P. Murcek, J. Teichert, and R. Xiang, "Building the Third SRF Gun at HZDR", in *Proc. IBIC'17*, Grand Rapids, MI, USA, Aug. 2017, pp. 98-100. doi:10.18429/JACoW-IBIC2017-MOPWC01
- [8] E. Vogel *et al.*, "SRF Gun Development at DESY", in *Proc. LINAC'18*, Beijing, China, Sep. 2018, pp. 105-108. doi:10.18429/JACoW-LINAC2018-MOP0037
- [9] D.H. Dowell and J.W. Lewellen, "Chapter 1: Photoinjector Theory," in *An Engineering Guide to Photoinjectors*, T. Rao and D.H. Dowell, Eds., 2013.
- [10] F. Sannibale, "High-brightness electron injectors for high-duty cycle X-ray free electron lasers," *Frontiers in Physics*, vol. 11, Jul. 2023. doi:10.3389/fphy.2023.1187346
- [11] S. P. Weathersby *et al.*, "Mega-electron-volt ultrafast electron diffraction at SLAC National Accelerator Laboratory," *Rev. Sci. Instrum.*, vol. 86, no. 7, Jul. 2015. doi:10.1063/1.4926994
- [12] D. Filippetto and H. Qian, "Design of a high-flux instrument for ultrafast electron diffraction and microscopy," *J. Phys. B: At. Mol. Opt. Phys.*, vol. 49, no. 10, p. 104003, Apr. 2016. doi:10.1088/0953-4075/49/10/104003
- [13] J. W. Lewellen *et al.*, "Status of the SLAC/MSU SRF Gun Development Project", in *Proc. NAPAC'22*, Albuquerque, NM, USA, Aug. 2022, pp. 623-626. doi:10.18429/JACoW-NAPAC2022-WEPA03
- [14] R. Akre *et al.*, "Commissioning the Linac Coherent Light Source injector," *Physical Review Special Topics - Accelerators and Beams*, vol. 11, no. 3, Mar. 2008. doi:10.1103/physrevstab.11.030703
- [15] <https://www.pulsar.nl/>
- [16] M. Borland, "ELEGANT: A flexible SDDS-compliant code for accelerator simulation," Office of Scientific and Technical Information (OSTI), Aug. 2000. doi:10.2172/761286.